Infrared Spectra of BCO, $B(CO)_2$, and OCBBCO in Solid Argon

Mingfei Zhou,*,†,‡ Nobuko Tsumori,† Lester Andrews,§ and Qiang Xu*,†

National Institute of Advanced Industrial Science and Technology (AIST), Ikeda, Osaka 563-8577, Japan, Shanghai Key Laboratory of Molecular Catalysts and Innovative Materials, Department of Chemistry & Laser Chemistry Institute, Fudan University, Shanghai 200433, P. R. China, and Department of Chemistry, University of Virginia, Charlottesville, Virginia 22901

Received: October 17, 2002; In Final Form: February 12, 2003

The reactions of ground-state boron atoms with CO in solid argon have been reinvestigated. The BCO molecule was formed by codeposition of laser-ablated boron atoms with CO in argon. The ν_1, ν_2, ν_3, $2\nu_1$, $2\nu_3$, and $\nu_1 + \nu_3$ modes of isotopic BCO molecules have been measured. The linear dicarbonyl, $B(CO)_2$, and the dimer OCBBCO were produced on sample annealing. Quantum chemical calculations of the geometry structures, vibrational frequencies, and intensities strongly support the experimental assignments. It is found that OCBBCO has a linear singlet ground state with some boron−boron triple-bond character. Bonding analysis shows that s to p (or σ to π) promotion plays a significant role in these boron carbonyl species.

Introduction

Main group element carbonyls have been the subject of considerable studies. The group 13 element carbonyls are among the most studied main group carbonyls both experimentally[1−11] and theoretically.[12−16] The neutral carbonyls of boron, aluminum, gallium, and indium have been prepared by cocondensation of thermally evaporated or laser-ablated element atoms with CO using the matrix isolation technique and detected and characterized using various spectroscopic methods such as infrared absorption and electron paramagnetic resonance.[1−11] There have also been a number of computational studies in predicting binding energies, structures, and harmonic vibrational frequencies of group 13 element carbonyls.[12−16]

Boron monocarbonyl was first studied by Hamrick et al. in solid neon and argon matrixes using electron spin resonance (ESR) spectroscopy.[6] The BCO molecule is quite different from the remaining group 13 element monocarbonyls. The ESR spectrum revealed that it has a quartet ground state with the three spins predominantly on the boron atom.[6] Burkholder and Andrews studied the infrared absorption spectra of the products resulting from the reaction of laser-ablated boron atoms and CO in solid argon.[7] The BCO and several higher order reaction products were assigned on the basis of observed C−O stretching vibrations. The BCO molecule and its isomers have been the subject of several quantum chemical calculations. Both ab initio and density functional calculations predicted that the BCO molecule has a $^4\Sigma$ ground state with linear structure, in good agreement with the experimental findings.[6,7,13,14] The BOC isomer was predicted to lie about 70 kcal/mol higher in energy than the $^4\Sigma$ ground-state BCO molecule at the SCF and MBPT levels.[6] The cyclic B(CO) isomer was predicted to have a doublet ground state and is about 28 kcal/mol less stable than the $^4\Sigma$ BCO molecule at MP2 level.[14]

It is noteworthy that most of the previous infrared measurements of main group element carbonyls were focused on the very intense absorptions associated with the C−O stretching vibrations. No M−CO stretching and bending vibrations have been reported for known group 13 element carbonyls, except $Al(CO)_2$.[4] As has been mentioned, the M−CO stretching and bending spectral information are important in description of the M−CO bonding and testing the quality of theoretical studies.[17] In this study, we report the results of a detailed matrix-isolation FTIR study of the reaction products formed between laser-ablated boron atoms and CO molecules in excess argon. We report here the frequencies of ν_1, ν_2, and ν_3 fundamentals and $2\nu_1$, $2\nu_3$, and $\nu_1+ \nu_3$ overtone or combination bands for BCO isotopomers. Meanwhile, some discrepancies that appeared on the previous identification of $B(CO)_2$ and OCBBCO are clarified. Our theoretical calculations found that OCBBCO exhibits some boron−boron triple-bond character. A preliminary report of the OCBBCO molecule has been communicated.[18]

Experimental and Computational Methods

The experimental setup is similar to those used previously.[19,20] The 1064 nm fundamental of a Nd:YAG laser was focused on a rotating boron target, and the laser-ablated boron atoms were codeposited with CO in excess argon onto a CsI window cooled normally to 8 K by means of a closed-cycle helium refrigerator. The matrix-gas deposition rate was typically of 2−4 mmol/h. Carbon monoxide, $^{13}C^{16}O$ (99% ^{13}CO, including 12% $^{13}C^{18}O$), and $^{12}C^{18}O$ (99%) were used to prepare the CO/Ar mixtures. Natural abundance boron (^{10}B, 19.8%; ^{11}B, 80.2%) and ^{10}B-enriched (97%) targets were used in different experiments. Matrix samples were deposited for 1−3 h. After sample deposition, IR spectra were recorded on a BIO-RAD FTS-6000e spectrometer at 0.5 cm^{-1} resolution using a liquid nitrogen cooled HgCdTe (MCT) detector for the spectral range of 5000−400 cm^{-1}.

Quantum chemical calculations were performed to predict the structures and vibrational frequencies of the observed reaction products using the Gaussian 98 program.[21] The Becke three-parameter hybrid functional with the Lee−Yang−Parr

* To whom correspondence should be addressed. E-mail addresses: mfzhou@fudan.edu.cn, q.xu@aist.go.jp.

† National Institute of Advanced Industrial Science and Technology (AIST).

‡ Fudan University.

§ University of Virginia.

10.1021/jp027229g CCC: $25.00
Published on Web 03/14/2003

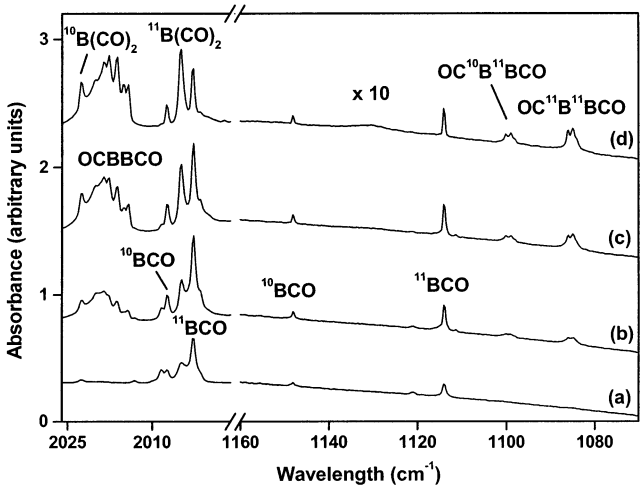

Figure 1. Infrared spectra in the 2026−1996 and 1160−1070 cm^{-1} regions from codeposition of laser-ablated natural abundance boron and 0.5% CO in Ar: (a) 1 h sample deposition at 8 K; (b) after 22 K annealing; (c) after 26 K annealing; (d) after 30 K annealing.

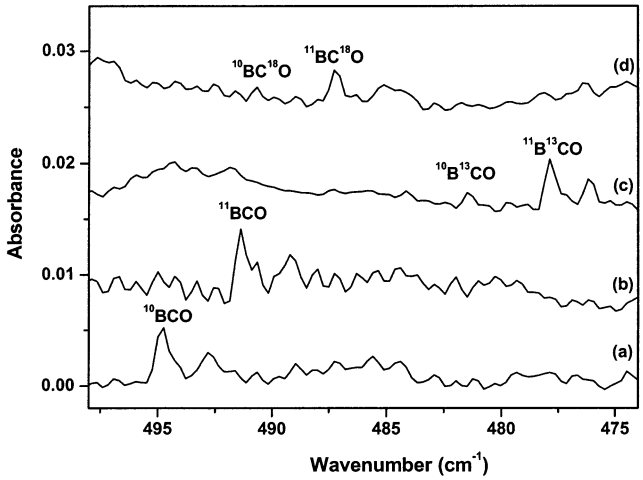

Figure 2. Infrared spectra in the 498−474 cm^{-1} region from codeposition of laser-ablated boron atoms with CO in excess argon (3 h sample deposition): (a) ^{10}B-enriched (97%) target, 1.5% $^{12}C^{16}O$; (b) natural abundance boron target, 1.5% $^{12}C^{16}O$; (c) natural abundance boron target, 1.5% $^{13}C^{16}O$; (d) natural abundance boron target, 1.5% $^{12}C^{18}O$.

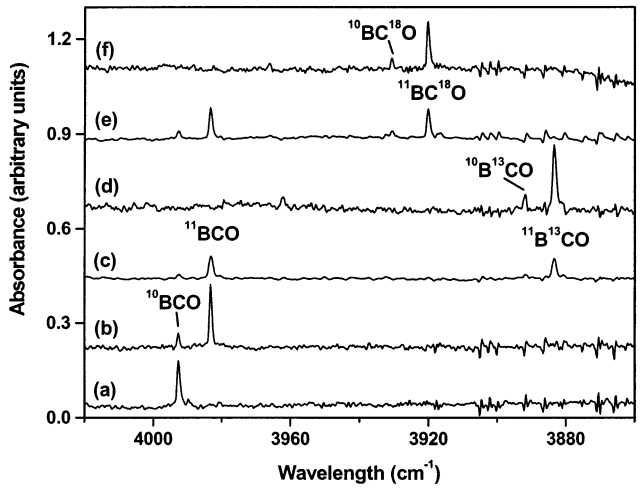

Figure 3. Infrared spectra in the 4020−3860 cm^{-1} region from codeposition of laser-ablated boron atoms with CO in excess argon: (a) ^{10}B-enriched (97%) target, 0.2% $^{12}C^{16}O$; (b) natural abundance boron target, 0.2% $^{12}C^{16}O$; (c) natural abundance boron target, 0.1% $^{12}C^{16}O$ + 0.1% $^{13}C^{16}O$; (d) natural abundance boron target, 0.2% $^{13}C^{16}O$ (containing 12% $^{13}C^{18}O$); (e) natural abundance boron target, 0.1% $^{12}C^{16}O$ + 0.1% $^{12}C^{18}O$; (f) natural abundance boron target, 0.2% $^{12}C^{18}O$.

correlation corrections (B3LYP) was used.[22,23] Comparative ab initio calculations were also performed at CCSD(T) level. The 6-311+G(d) basis sets were used for B, C, and O atoms.[24,25] Geometries were fully optimized and vibrational frequencies calculated with analytical second derivatives.

Results and Discussion

Infrared Spectra. Series of experiments have been done using different CO concentrations and different laser energies. Here, we report the results with relatively high CO concentrations (ranging from 0.1% to 1.5%) and low laser energies (typically 5−10 mJ/pulse). Figure 1 shows the infrared spectra in the C−O and B−C stretching vibrational regions from codeposition of laser-ablated boron atoms (with natural abundance boron target) with 0.5% CO at 8 K and then annealing of the sample to different temperatures. The infrared spectra in the C−O stretching frequency region are about the same as that previously reported.[7] After 1 h of sample deposition at 8 K, the matrix sample displayed strong absorptions at 2002.6 and 2007.3 cm^{-1}. These correspond to the absorptions reported at 2002.5 and 2007.2 cm^{-1} that were previously assigned to the C−O stretching vibration of ^{11}BCO and ^{10}BCO, respectively.[7] Annealing the matrix to 22 and 26 K caused these bands to increase and several new bands at 2004.9, 2022.5, 2014.2, and 2016.1 cm^{-1} to appear. The 2004.9 and 2022.5 cm^{-1} bands are sharp and have been assigned previously to the OCBBCO dimer.[7] The 2014.2 and 2016.1 cm^{-1} bands have been assigned previously to $B(CO)_2$. These new bands all increased on subsequent annealing of the matrix to high temperatures, as shown in Figure 1. When ^{10}B-enriched target was used, only the 2007.3 cm^{-1} band was presented on the spectrum after sample deposition and the 2022.5 cm^{-1} band appeared on annealing. The 2014.2 and 2016.1 cm^{-1} bands shifted to 2016.4 and 2018.3 cm^{-1}.

Besides the product absorptions in the C−O stretching vibrational region, several new absorptions were also observed. The spectra in different regions are shown in Figures 1−5. Five pairs of weak absorptions at 494.8/491.3, 1148.1/1114.1, 2291.1/2225.0, 3139.1/3099.7, and 3992.7/3983.2 cm^{-1} exhibited the same growth or decay characteristics as the strong C−O stretching vibration of BCO observed at 2007.3/2002.6 cm^{-1} upon matrix annealing in different CO concentration and different laser power experiments. This indicated that these absorptions are due to the same molecule, that is, BCO. The relative intensities between high- and low-frequency absorptions for each pair match the natural abundance of boron (19.8% ^{10}B, 80.2% ^{11}B). When ^{10}B-enriched target was used, only the high-frequency bands were observed for each pair.

A doublet at 1116.5/1114.9 cm^{-1} was produced on annealing after the BCO absorptions in the experiments with ^{10}B-enriched target. When natural abundance boron target was used, two doublets at 1100.1/1098.9 and 1086.1/1084.9 cm^{-1} appeared together on annealing. The upper doublet is about 50% in intensity of the lower doublet, and the relative intensities kept in constant through all of the experiments. These doublets tracked the 2014.2/2016.1 cm^{-1} bands in the C−O stretching frequency region, suggesting that they are due to the same species.

The experiments were repeated using isotopically labeled $^{13}C^{16}O$ and $^{12}C^{18}O$ and $^{12}C^{16}O$ + $^{13}C^{16}O$ and $^{12}C^{16}O$ + $^{12}C^{18}O$ mixtures. The spectra in selected regions are also shown in Figures 2−5, and the absorptions are summarized in Tables 1 and 2.

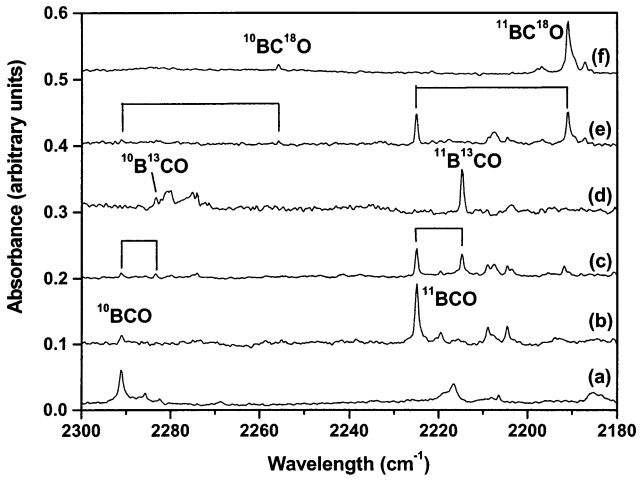

Figure 4. Infrared spectra in the 2300−2180 cm^{-1} region from codeposition of laser-ablated boron atoms with CO in excess argon: (a) ^{10}B-enriched (97%) target, 0.2% $^{12}C^{16}O$; (b) natural abundance boron target, 0.2% $^{12}C^{16}O$; (c) natural abundance boron target, 0.1% $^{12}C^{16}O$ + 0.1% $^{13}C^{16}O$; (d) natural abundance boron target, 0.2% $^{13}C^{16}O$ (containing 12% $^{13}C^{18}O$); (e) natural abundance boron target, 0.1% $^{12}C^{16}O$ + 0.1% $^{12}C^{18}O$; (f) natural abundance boron target, 0.2% $^{12}C^{18}O$.

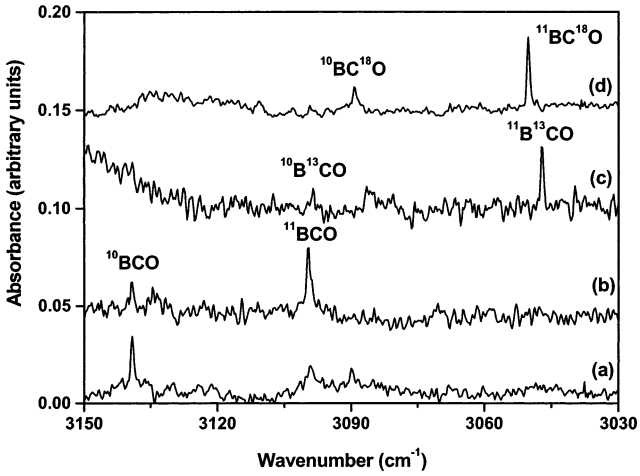

Figure 5. Infrared spectra in the 3150−3030 cm^{-1} region from codeposition of laser-ablated boron atoms with CO in excess argon: (a) ^{10}B-enriched (97%) target, 0.2% $^{12}C^{16}O$; (b) natural abundance boron target, 0.2% $^{12}C^{16}O$; (c) natural abundance boron target, 0.2% $^{13}C^{16}O$ (containing 12% $^{13}C^{18}O$); (d) natural abundance boron target, 0.2% $^{12}C^{18}O$.

TABLE 1: Vibrational Frequencies (cm^{-1}) and Relative Intensities of the IR Bands Observed for Various BCO Isotopomers

^{10}B			^{11}B			
$^{12}C^{16}O$	$^{13}C^{16}O$	$^{12}C^{18}O$	$^{12}C^{16}O$[a]	$^{13}C^{16}O$	$^{12}C^{18}O$	assignment
3992.7	3891.7	3930.6	3983.2 (2.1)	3883.5	3920.2	$2\nu_1$
3139.1	3086.7	3089.4	3099.7 (0.3)	3047.2	3050.2	$\nu_1+\nu_3$
2291.1	2283.3	2255.8	2225.0 (0.7)	2214.7	2190.9	$2\nu_3$
2007.3	1956.5	1975.9	2002.6 (22)	1952.2	1970.7	ν_1
1148.1	1144.7	1130.0	1114.1 (1)	1109.8	1096.5	ν_3
494.8	481.3	490.7	491.3(0.07)	477.9	487.2	ν_2

[a] Values in parentheses are IR intensities normalized to the ν_3 fundamental.

Calculation Results. Calculations on the $^4\Sigma^-$ state of linear BCO were conducted at the B3LYP and CCSD(T) levels of theory. The optimized geometric parameters are shown in Figure 6. The B−C bond length predicted by the B3LYP functional is slightly shorter than that predicted by the CCSD(T) method. But the C−O bond length is predicted to be almost the same.

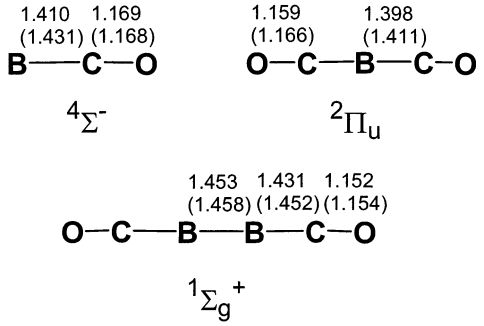

Figure 6. Optimized structures of BCO, $B(CO)_2$, and OCBBCO at B3LYP/6-311+G(d) and CCSD(T)/6-311+G(d) (in parentheses) levels of theory. Bond lengths are given in Å.

Calculations were also done on the $B(CO)_2$ and OCBBCO molecules, and the optimized geometric parameters are also shown in Figure 6. In contrast to the previous SCF calculations, which predicted a bent structure, the present calculations found that the $B(CO)_2$ molecule is linear.[7] As will be discussed, our experimental data also suggest the molecule to be linear. The SCF level of theory previously employed is probably insufficient in describing this molecule.

BCO. As has been discussed in detail previously,[7] the 2007.3 and 2002.6 cm^{-1} bands are due to the C−O stretching (ν_1) vibrations of ^{10}BCO and ^{11}BCO. Besides the C−O stretching vibration, five pairs of bands were also observed in the present experiments, which are also due to BCO absorptions. The 1148.1 and 1114.1 cm^{-1} bands are assigned to the B−CO stretching (ν_3) vibration of ^{10}BCO and ^{11}BCO. These two bands shifted to 1144.7 and 1109.8 cm^{-1} with $^{13}C^{16}O$, and to 1130.0 and 1096.5 cm^{-1} with $^{12}C^{18}O$. In the mixed $^{12}C^{16}O$ + $^{13}C^{16}O$ and $^{12}C^{16}O$ + $^{12}C^{18}O$ experiments, no intermediate component was observed, indicating that there is only one CO in the molecule. The very weak bands at 494.8 and 491.3 cm^{-1} are assigned to the bending (ν_2) vibration of ^{10}BCO and ^{11}BCO.

The remaining three band pairs at 3992.7/3983.2, 3139.1/3099.7, and 2291.1/2225.0 cm^{-1} are too high for vibrational fundamentals of BCO, and overtone or combination modes must be considered. The 3992.7/3983.2 cm^{-1} bands are assigned to the $2\nu_1$ overtone vibration of ^{10}BCO and ^{11}BCO, respectively. These two bands shifted to 3891.7 and 3883.5 cm^{-1} with $^{13}C^{16}O$ and to 3930.6 and 3920.2 cm^{-1} with $^{12}C^{18}O$. The isotopic $^{10}B/^{11}B$ ratio (1.0024), $^{12}C/^{13}C$ ratios (^{10}B, 1.0260; ^{11}B, 1.0257), and $^{16}O/^{18}O$ ratios (^{10}B, 1.0158; ^{11}B, 1.0161) are almost exactly the same as those observed for the ν_1 fundamental ($^{10}B/^{11}B$, 1.0023; $^{12}C/^{13}C$, 1.0260, 1.0258; $^{16}O/^{18}O$, 1.0159, 1.0162) and strongly support the overtone assignment. For $^{10}B^{12}C^{16}O$, $2\nu_1 = 4014.6$ cm^{-1}, while for $^{11}B^{12}C^{16}O$, $2\nu_1 = 4005.2$ cm^{-1}. The anharmonicity constant was deduced to be -11.0 cm^{-1}.

The band positions of the 2291.1 and 2225.0 cm^{-1} absorptions are appropriate for a $2\nu_3$ overtone. For $^{10}B^{12}C^{16}O$, $2\nu_3 = 2296.2$ cm^{-1}, and for $^{11}B^{12}C^{16}O$, $2\nu_3 = 2228.2$ cm^{-1}, which gave 5.1 and 3.2 cm^{-1} differences from the observed absorptions. The isotopic frequency shifts also provide good support. Taking the 2225.0 cm^{-1} band, for example, it shifted to 2214.7 cm^{-1} with $^{13}C^{16}O$ and to 2190.9 cm^{-1} with $^{12}C^{18}O$, which gave isotopic $^{12}C/^{13}C$ and $^{16}O/^{18}O$ ratios of 1.0047 and 1.0156, respectively. These isotopic ratios of the ν_3 fundamental were experimentally deduced to be 1.0039 and 1.0161.

The much weaker absorptions at 3139.1 and 3099.7 cm^{-1} are assigned to $\nu_1 + \nu_3$ combination bands of ^{10}BCO and ^{11}BCO, respectively. For $^{10}B^{12}C^{16}O$, $\nu_1 + \nu_3 = 3155.4$ cm^{-1}, which is just 16.3 cm^{-1} higher than the band observed at 3139.1 cm^{-1}. For $^{11}B^{12}C^{16}O$, $\nu_1 + \nu_3 = 3116.7$ cm^{-1}, which is about 17.0

TABLE 2: Observed and Calculated Symmetric and Antisymmetric CO Stretching Vibrational Frequencies (cm^{-1}) for $B(CO)_2$[a]

	^{10}B				^{11}B			
	obsd		calcd		obsd		calcd	
	sym	asym	sym	asym	sym	asym	sym	asym
$B(CO)_2$		2022.5	2149.2	2112.3		2004.9	2149.2	2097.4
$B(^{12}CO)(^{13}CO)$	2059.0	1989.3	2135.5	2071.9	2055.8	1974.4	2132.7	2059.3
$B(^{13}CO)_2$		1976.8	2092.3	2060.8		1959.6	2092.3	2045.1
$B(C^{16}O)(C^{18}O)$	2072.4	2007.4	2136.5	2094.1	2070.5	1988.9	2135.1	2079.5
$B(C^{18}O)_2$		1993.9	2110.8	2088.7		1977.7	2110.8	2071.5

[a] The calculated IR intensities of symmetric and antisymmetric CO stretching modes are as follows: $^{11}B(CO)_2$, 0 and 2709 km/mol; $^{11}B(^{12}CO)(^{13}CO)$, 452 and 2190 km/mol; $^{11}B(C^{16}O)(C^{18}O)$, 242 and 2429 km/mol. The other modes of $^{11}B(CO)_2$ were predicted at 1489.2 cm^{-1} (σ_u, 2 km/mol), 637.3 (σ_g, 0 km/mol), 524.0 (π_u, 62 km/mol), 504.0 (π_g, 0 km/mol), and 80.9 (π_u, 2 km/mol).

TABLE 3: Comparisons between Experimental and Calculated Vibrational Frequencies and Isotopic Frequency Ratios of ^{11}BCO

mode	method	freq[a]	$R(^{10}B/^{11}B)$	$R(^{12}C/^{13}C)$	$R(^{16}O/^{18}O)$
ν_1	B3LYP	2048.6 (405)	1.0021	1.0268	1.0163
	CCSD(T)	2049.4	1.0018	1.0265	1.0172
	exptl	2002.6	1.0023	1.0258	1.0159
ν_3	B3LYP	1130.6 (14)	1.0329	1.0010	1.0179
	CCSD(T)	1096.3	1.0333	1.0013	1.0171
	exptl	1114.1	1.0305	1.0039	1.0161
ν_2	B3LYP	483.4 (1)	1.0077	1.0285	1.0088
	CCSD(T)	489.5	1.0078	1.0277	1.0089
	exptl	491.3	1.0071	1.0280	1.0084

[a] Values in parentheses are calculated intensities in km/mol.

cm^{-1} higher than the band observed at 3099.7 cm^{-1}. The boron isotopic shift of 39.4 cm^{-1} is about the same with the sum of the isotopic shifts observed for the ν_1 (4.7 cm^{-1}) and ν_3 (34.0 cm^{-1}) fundamentals. These two bands shifted to 3086.7 and 3047.2 cm^{-1} with $^{13}C^{16}O$, and to 3089.4 and 3050.2 cm^{-1} with $^{12}C^{18}O$, respectively. The observed isotopic $^{12}C/^{13}C$ shifts (52.4 and 52.5 cm^{-1}) and $^{16}O/^{18}O$ shifts (49.7 and 49.5 cm^{-1}) correlate very well with the sum of the observed isotopic shifts of the ν_1 and ν_3 fundamentals ($^{12}C/^{13}C$, 54.2 and 54.7 cm^{-1}; $^{16}O/^{18}O$, 49.5 and 49.5 cm^{-1}).

Agreement between the band positions calculated for $^{11}B^{12}C^{16}O$ (Table 3) and the observed fundamentals is excellent at both levels of theory. B3LYP calculations predicted that the ν_1, ν_2, and ν_3 modes of BCO exhibit 405:1:14 relative intensities. Experimentally, we got roughly 330:1:15 relative intensities. Because isotopic frequency shifts are more sensitive indicators of the description of normal vibrational modes, we evaluated the experimentally observed and calculated isotopic frequency ratios for the observed modes, and the results are listed in Table 3. In general, agreements between observed and calculated ratios are good at both levels of theory. However, the ν_1 and ν_2 modes fit better than the ν_3 mode. As can be seen in Table 3, the calculated isotopic frequency ratios for the ν_1 and ν_2 modes fit the experimental values very well, but the calculated $^{12}C/^{13}C$ ratios for the ν_3 mode are smaller than the observed ratios. It is interesting to note that the experimental $^{12}C/^{13}C$ ratio of ^{10}BCO (1.0030) is larger than that of ^{11}BCO (1.0039) when the frequency is higher. This suggests the possibility of an anharmonic resonance of the B−CO stretch with the bending vibration (ν_2) with a relatively larger $^{12}C/^{13}C$ isotopic effect. Although the ν_3 and $2\nu_2$ levels are quite different, anharmonic resonance between ν_3 and $2\nu_2$ should be considered here. As a reference point, the ν_3 (859 cm^{-1}) and $2\nu_2$ (1040 cm^{-1}) of SCO are quite far apart, but resonance still takes place. [27, 28]

The $^4\Sigma^-$ ground state of BCO has an electron configuration of $(1\sigma)^2\ (2\sigma)^2\ (3\sigma)^2\ (4\sigma)^2\ (5\sigma)^2\ (6\sigma)^2\ (1\pi)^4\ (7\sigma)^1\ (2\pi)^2$, which reflects the B $2s^1\ 2p^2$ excited state (^4P). The three unpaired electrons occupy the 7σ and 2π molecular orbitals. The 7σ molecular orbital is largely B 2s in character and is nonbonding. The doubly degenerate 2π molecular orbitals are largely B 2p in character and comprise B 2p → CO 2π back-bonding. The formation of $^4\Sigma^-$ state BCO from ground-state B (^2P) and CO involves B 2s → 2p promotion, which requires about 82.5 kcal/mol promotion energy.[26] This promotion increases the B−CO bonding by decreasing the σ repulsion and increasing the B 2p → CO 2π back-bonding.

$B(CO)_2$. In natural abundance boron experiments, absorptions at 2022.5 and 2004.9 cm^{-1} appeared together on annealing. When the ^{10}B-enriched boron target was used, only the 2022.5 cm^{-1} band was observed. The 2022.5 cm^{-1} band is about $^1/_4$ intensity of the 2004.9 cm^{-1} band, which clearly indicates that only one boron atom is involved in this mode. These two bands shifted to 1976.8 and 1959.6 cm^{-1} with $^{13}C^{16}O$ and to 1993.9 and 1977.7 cm^{-1} with $^{12}C^{18}O$ and gave isotopic $^{12}C/^{13}C$ ratios of 1.0231 and 1.0231 and $^{16}O/^{18}O$ ratios of 1.0143 and 1.0138, respectively. The $^{10}B/^{11}B$ ratio (1.0088) is higher than that for BCO, and the $^{12}C/^{13}C$ ratios are lower than those for BCO, indicating more boron and less C involvement in this vibrational mode. In the mixed $^{12}C^{16}O + {}^{13}C^{16}O$ experiments, triplets were observed for both bands with intermediates at 1989.3 and 1974.4 cm^{-1}, indicating that two equivalent C atoms are involved. Similar triplets with intermediates at 2007.4 and 1988.9 cm^{-1} were also observed in the mixed $^{12}C^{16}O + {}^{12}C^{18}O$ experiments, which indicate that two equivalent O atoms are involved. Accordingly, the 2022.5 and 2004.9 cm^{-1} bands are assigned to the antisymmetric C−O stretching vibrations of the linear $^{10}B(CO)_2$ and $^{11}B(CO)_2$ molecules, respectively. The symmetric C−O stretching mode of linear $B(CO)_2$ is IR inactive, but this mode of the $B(^{12}CO)(^{13}CO)$ and $B(C^{16}O)(C^{18}O)$ molecules is IR active because of the reduced symmetry. Two weak new bands at 2059.0 and 2055.8 cm^{-1} were observed in the mixed $^{12}C^{16}O + {}^{13}C^{16}O$ experiment and track with the 2022.5 and 2004.9 cm^{-1} bands. These two bands are the symmetric C−O stretching modes of the $^{10}B(^{12}CO)(^{13}CO)$ and $^{11}B(^{12}CO)(^{13}CO)$ molecules. The symmetric C−O stretching modes of the $^{10}B(C^{16}O)(C^{18}O)$ and $^{11}B(C^{16}O)(C^{18}O)$ molecules were observed at 2072.4 and 2070.5 cm^{-1}, respectively. The weak 4078.7 and 4061.1 cm^{-1} bands are assigned to the combination bands of the linear $^{10}B(CO)_2$ and $^{11}B(CO)_2$ molecules. These two bands are separated from the 2022.5 and 2004.9 cm^{-1} bands both by 2056.2 cm^{-1}. This frequency separation is appropriate for a symmetric C−O stretching vibration. Taking the anharmonicity into consideration, the symmetric C−O stretching mode of $B(CO)_2$ should be around 2080 cm^{-1}. The combination bands were observed at 3978.8 and 3962.0 cm^{-1} with ^{13}CO and at 4020.2 and 3999.5 cm^{-1} with $C^{18}O$.

The assignment is strongly supported by theoretical calculations. As noted above, our theoretical calculations found a $^2\Pi_u$ ground state for $B(CO)_2$ with a linear structure. The antisym-

metric C−O stretching vibration for $^{11}B(CO)_2$ was calculated at 2097.4 cm^{-1} at B3LYP/6-311+G(d) level of theory. As listed in Table 2, the calculated $^{10}B/^{11}B$ ratio, $^{12}C/^{13}C$ ratios, and $^{16}O/^{18}O$ ratios are all in good agreement with the experimental observations. The IR inactive symmetric C−O stretching mode was predicted at 2150.2 cm^{-1} for both $^{10}B(CO)_2$ and $^{11}B(CO)_2$. The symmetric C−O stretching modes for $^{10}B(^{12}CO)(^{13}CO)$ and $^{11}B(^{12}CO)(^{13}CO)$ were predicted at 2136.4 and 2133.6 cm^{-1} with appreciable intensities. Similar modes for $^{10}B(C^{16}O)(C^{18}O)$ and $^{11}B(C^{16}O)(C^{18}O)$ were predicted at 2137.4 and 2136.0 cm^{-1}. We also predicted a B−C stretching mode at 1489.7 cm^{-1} with a much lower intensity (2 km/mol). This mode was not observed experimentally.

The 2004.9 and 2022.5 cm^{-1} bands correspond to the absorptions reported at 2004.6 and 2022.2 cm^{-1} that were previously assigned to the C−O stretching vibration of a $(BCO)_2$ molecule, which was in error.[7] As will be discussed, absorptions at 2014.2/2016.1 cm^{-1}, which have been assigned previously to $B(CO)_2$, are due to OCBBCO absorptions. The CO concentration experiments also support the assignment. Compared to the BCO and the OCBBCO absorptions, the 2004.9 and 2022.5 cm^{-1} absorptions are strong in experiments with high CO concentrations but are very weak in experiments with low CO concentrations. In the experiments with relatively low CO concentration and high ablation laser energy, some boron cluster species, BBCO and $B_4(CO)_2$, were formed.[29]

According to our calculations, the ground state of $B(CO)_2$ reflects the B $2p^3$ electron configuration of the B atom. Formation of $B(CO)_2$ from quartet BCO and CO requires BCO $7\sigma \rightarrow 2\pi$ promotion. The molecule is predicted to have a $^2\Pi_u$ ground state with an electron configuration of $...(6\sigma_g)^2\ (5\sigma_u)^2\ (1\pi_u)^4\ (1\pi_g)^4\ (2\pi_u)^3$. The doubly degenerate $2\pi_u$ HOMOs are largely B p_π orbitals, which comprise significant B 2p → CO 2π back-bonding. The doubly degenerate $1\pi_g$ HOMO-1 and $1\pi_u$ HOMO-2 are primary C−O π bonding orbitals. The $5\sigma_u$ HOMO-3 and the $6\sigma_g$ HOMO-4 are CO → B σ donation orbitals.

OCBBCO. A split band at 1116.5/1114.9 cm^{-1} in ^{10}B-enriched experiments and two split bands at 1100.1/1098.9 and 1086.1/1084.9 cm^{-1} in natural abundance experiments are assigned to the B−C stretching vibrations of the $OC^{10}B^{10}BCO$, $OC^{10}B^{11}BCO$, and $OC^{11}B^{11}BCO$ molecules at two trapping sites.[18] The relative intensities of these absorptions are consistent with two equivalent boron atom involvements. In the mixed $^{12}C^{16}O + ^{13}C^{16}O$ and $^{12}C^{16}O + ^{12}C^{18}O$ experiments, each band splits into a triplet with approximately 1:2:1 relative intensities, indicating that two equivalent C atoms and two equivalent O atoms are involved in this mode. The split band at 2014.2/2016.1 cm^{-1} in natural abundance boron experiments and the split band at 2016.4/2018.3 cm^{-1} in ^{10}B-enriched experiments are due to C−O stretching vibrations of the $OC^{11}B^{11}BCO$ and $OC^{10}B^{10}BCO$ molecules. As has been discussed in detail previously,[7] these bands split into triplets in the mixed $^{12}C^{16}O + ^{13}C^{16}O$ and $^{12}C^{16}O + ^{12}C^{18}O$ experiments, indicating that two equivalent CO molecules are involved. In low-frequency region, weak bands at 521.4 and 517.1 cm^{-1} are assigned to the BCO bending vibrations of the $OC^{10}B^{10}BCO$ and $OC^{11}B^{11}BCO$ molecules. The boron isotopic splittings in natural abundance boron experiments could not be resolved for the C−O stretching and BCO bending modes because of site splittings.

OCBBCO was predicted to have a singlet ground state with linear geometry (Figure 6). The dominant configuration of the ground-state OCBBCO is $...(6\sigma_g)^2\ (6\sigma_u)^2\ (1\pi_u)^4\ (1\pi_g)^4\ (7\sigma_g)^2\ (2\pi_u)$.[4] The molecule can be viewed as the interaction of a closed-shell excited state ($^1\Sigma_g^+$) B_2 in the $(1\sigma_g)^2\ (1\sigma_u)^2\ (2\sigma_g)^2\ (1\pi_u)^4\ (2\sigma_u)^0\ (3\sigma_g)^0$ configuration and two CO's. Because closed-shell excited state ($^1\Sigma_g^+$) B_2 is a typical boron−boron triple-bonded molecule, singlet OCBBCO exhibits some boron−boron triple-bond character. The ground state of B_2 molecule is $^3\Sigma_g^-$ with electron configuration of $(1\sigma_g)^2\ (1\sigma_u)^2\ (2\sigma_g)^2\ (2\sigma_u)^2\ (1\pi_u)^2$; the formal addition of two CO's to form OCBBCO involves two $\sigma_u \rightarrow \pi_u$ promotions.

The bonding in BCO, $B(CO)_2$, and OCBBCO exhibits marked difference from the remaining group 13 metal carbonyls. Although the s → p promotion energy decreases down the group, it is not compensated by the increased metal−CO bonding interaction. The monocarbonyls of heavier group 13 metals all have doublet ground states.[11] Similar conclusions can also be drawn for dicarbonyls. The ground states of $Al(CO)_2$, $Ga(CO)_2$, and $In(CO)_2$ dicarbonyls reflect the s^2p^1 ground electron configurations of the metal atoms and are highly bent to reduce the σ repulsion. Formation of the linear boron−boron multiply bonded OCBBCO is unique for boron. No similar species has been observed for the remaining group 13 carbonyls. A recent matrix-isolation FTIR spectroscopic study has shown that the Ga + CO reaction gave the dibridged $Ga_2(CO)_2$ gallium carbonyl.[11] No $Al_2(CO)_2$ species has been observed in the solid argon matrix studies,[4] but recent investigation has characterized the dibridged $Al_2(CO)_2$ carbonyl in solid neon.[30]

Conclusions

The infrared absorption spectra of BCO, $B(CO)_2$, and OCBBCO have been measured. The BCO molecules have been produced via reactions of ground-state boron atoms with CO molecules in solid argon matrix and characterized by isotopic substitutions, as well as density functional theory calculations. The ν_1, ν_2, ν_3, $2\nu_1$, $2\nu_3$, and $\nu_1 + \nu_3$ vibrations of the isotopic BCO molecules have been reported. The dicarbonyl $B(CO)_2$ molecules were produced on annealing. It was predicted to have a $^2\Pi_u$ ground state with linear structure. The OCBBCO molecules were also formed via BCO dimerization.

The bonding in boron carbonyls is very different from that of the remaining group 13 element carbonyls. The boron carbonyls are linear molecules and their bonding involves significant B s → p or $\sigma \rightarrow \pi$ promotions. Although the s → p promotion energy decreases down the group, it is not compensated by the increased metal−CO bonding interaction in the heavier group 13 metal carbonyls. As a result, the BCO molecule has a quartet ground state, while the heavy element monocarbonyls have doublet ground states. The $B(CO)_2$ molecule is linear, but the $Al(CO)_2$, $Ga(CO)_2$, and $In(CO)_2$ dicarbonyls are highly bent to reduce the σ repulsion. Of particular interest, the BCO molecules prefer to form a linear boron−boron bonded dimer, whereas a bridge-bonded structure was favored for $Al_2(CO)_2$ and $Ga_2(CO)_2$.

Acknowledgment. We thank the referees for helpful discussions. This work is supported by NSFC (Grants 20003003 and 20125033), the NKBRSF of China, and the NEDO of Japan.

References and Notes

(1) Hinchcliffe, A. J.; Ogden, J. S.; Oswald, D. D. *J. Chem. Soc., Chem. Commun.* **1972**, 338.

(2) Kasai, P. H.; Jones, P. M. *J. Am. Chem. Soc*. **1984**, *106*, 8018. Chenier, J. H. B.; Hampson, C. A.; Howard, J. A.; Mile, B.; Sutcliffe, R. *J. Phys. Chem*. **1986**, *90*, 1524.

(3) Chenier, J. H. B.; Hampson, C. A.; Howard, J. A.; Mile, B. *J. Chem. Soc., Chem. Commun*. **1986**, 730.

(4) Xu, C.; Manceron, L.; Perchard, J. P. *J. Chem. Soc., Faraday Trans*. **1993**, *89*, 1291.

(5) Feltrin, A.; Guido, M.; Cesaro, S. N. *Vib. Spectrosc*. **1995**, *8*, 175.
(6) Hamrick, Y. M.; Van Zee, R. J.; Godbout, J. T.; Weltner, W.; Lauderdale, W. J.; Stanton, J. F.; Bartlett, R. J. *J. Phys. Chem*. **1991**, *95*, 2840.
(7) Burkholder, T. R.; Andrews, L. *J. Phys. Chem*. **1992**, *96*, 10195.
(8) Zhang, L. N.; Dong, J.; Zhou, M. F.; Qin, Q. Z. *J. Chem. Phys.* **2000**, *113*, 10169.
(9) Howard, J. A.; Sutcliffe, R.; Hampson, C. A.; Mile, B. *J. Phys. Chem*. **1986**, *90*, 4268.
(10) Kasai, P. H.; Jones, P. M. *J. Phys. Chem*. **1985**, *89*, 2019. Hatton, W. G.; Hacker, N. P.; Kasai, P. H. *J. Phys. Chem*. **1989**, *93*, 1328.
(11) Himmel, H. J.; Downs, A. J.; Green, J. C.; Greene, T. M. *J. Phys. Chem. A* **2000**, *104*, 3642.
(12) Balaji, V.; Sunil, K. K.; Jordan, K. D. *Chem. Phys. Lett.* **1987**, *136*, 309.
(13) Bridgeman, A. J. *J. Chem. Soc., Dalton Trans.* **1997**, 1323. Bridgeman, A. J. *Inorg. Chim. Acta*. **2001**, *321*, 27.
(14) Skancke, A.; Liebman, J. F. *J. Phys. Chem*. **1994**, *98*, 13215.
(15) Wesolowski, S. S.; Crawford, T. D.; Fermann, J. T.; Schaefer, H. F. *J. Chem. Phys*. **1996**, *104*, 3672. Wesolowski, S. S.; Galbraith, J. M.; Schaefer, H. F. *J. Chem. Phys.* **1998**, *108*, 9398.
(16) Jursic, B. S. *Chem. Phys*. **1997**, *219*, 57.
(17) Krim, L.; Alikhani, E. M.; Manceron, L. *J. Phys. Chem. A* **2001**, *105*, 7812. Tremblay, B.; Manceron, L. *Chem. Phys*. **1999**, *250*, 187.
(18) Zhou, M. F.; Tsumori, N.; Andrews, L.; Xu, Q. *J. Am. Chem. Soc*. **2002**, *124*, 12936.
(19) Burkholder, T. R.; Andrews, L. *J. Chem. Phys*. **1991**, *95*, 8697.
(20) Chen, M. H.; Wang, X. F.; Zhang, L. N.; Yu, M.; Qin, Q. Z. *Chem. Phys*. **1999**, *242*, 81.
(21) Frisch, M. J.; Trucks, G. W.; Schlegel, H. B.; Scuseria, G. E.; Robb, M. A.; Cheeseman, J. R.; Zakrzewski, V. G.; Montgomery, J. A., Jr.; Stratmann, R. E.; Burant, J. C.; Dapprich, S.; Millam, J. M.; Daniels, A. D.; Kudin, K. N.; Strain, M. C.; Farkas, O.; Tomasi, J.; Barone, V.; Cossi, M.; Cammi, R.; Mennucci, B.; Pomelli, C.; Adamo, C.; Clifford, S.; Ochterski, J.; Petersson, G. A.; Ayala, P. Y.; Cui, Q.; Morokuma, K.; Malick, D. K.; Rabuck, A. D.; Raghavachari, K.; Foresman, J. B.; Cioslowski, J.; Ortiz, J. V.; Stefanov, B. B.; Liu, G.; Liashenko, A.; Piskorz, P.; Komaromi, I.; Gomperts, R.; Martin, R. L.; Fox, D. J.; Keith, T.; Al-Laham, M. A.; Peng, C. Y.; Nanayakkara, A.; Gonzalez, C.; Challacombe, M.; Gill, P. M. W.; Johnson, B. G.; Chen, W.; Wong, M. W.; Andres, J. L.; Head-Gordon, M.; Replogle, E. S.; Pople, J. A. *Gaussian 98*, revision A.7; Gaussian, Inc.: Pittsburgh, PA, 1998.
(22) Becke, A. D. *J. Chem. Phys.* **1993**, *98*, 5648.
(23) Lee, C.; Yang, E.; Parr, R. G. *Phys. Rev. B* **1988**, *37*, 785.
(24) McLean, A. D.; Chandler, G. S. *J. Chem. Phys.* **1980**, *72*, 5639. Krishnan, R.; Binkley, J. S.; Seeger, R.; Pople, J. A. *J. Chem. Phys.* **1980**, *72*, 650.
(25) Wachter, J. H. *J. Chem. Phys.* **1970**, *52*, 1033. Hay, P. J.; Wadt, W. R. *J. Chem. Phys.* **1985**, *82*, 299.
(26) Radzig, A. A.; Smirnov, B. M. *Reference Data on Atoms, Molecules and Ions*; Springer-Verlag: Berlin, 1985.
(27) Morino, Y.; Nakagawa, T. *J. Mol. Spectrosc*. **1968**, *26*, 496.
(28) Foord, A.; Smith, J. G.; Whiffen, D. H. *Mol. Phys.* **1975**, *29*, 1685.
(29) Zhou, M. F.; Xu, Q.; Wang, Z. X.; Schleyer, P. v. R. *J. Am. Chem. Soc*. **2002**, *124*, 14854.
(30) Kong, Q. Y.; Chen, M. H.; Dong, J.; Li, Z. H.; Fan, K. N.; Zhou, M. F. *J. Phys. Chem. A* **2002**, *106*, 11709.